Environmental Science & Technology

Article

pubs.acs.org/est

Exploring the Use of Molecular Docking to Identify Bioaccumulative Perfluorinated Alkyl Acids (PFAAs)

Carla A. Ng* and Konrad Hungerbuehler

Institute for Chemical and Bioengineering, ETH Zurich, CH-8093 Zurich, Switzerland

Supporting Information

ABSTRACT: Methods to predict the bioaccumulation potential of per- and polyfluorinated alkyl substances (PFAS) are sorely needed, given the proliferation of these substances and lack of data on their properties and behavior. Here, we test whether molecular docking, a technique where interactions between proteins and ligands are simulated to predict both bound conformation and interaction affinity, can be used to predict PFAS binding strength and biological half-life. We show that an easy-to-implement docking program, Autodock Vina, can successfully redock perfluorooctanesulfonate (PFOS) to human serum albumin with deviations smaller than 2 Å. Furthermore, predicted binding strengths largely fall within one standard deviation of measured values for perfluorinated alkyl acids (PFAAs). Correlations with half-lives suggest both membrane partitioning and protein interactions are important, and that serum albumin is only one of a number of proteins controlling the fate of these chemicals in organisms. However, few data are available for validation of our approach as a broad screening tool, and available data are highly variable. We therefore call for collection of new data, particularly including proteins other than serum albumin and substances beyond perfluorooctanoic acid (PFOA) and PFOS. The methods we discuss in this work can serve as a framework for guiding such data collection.

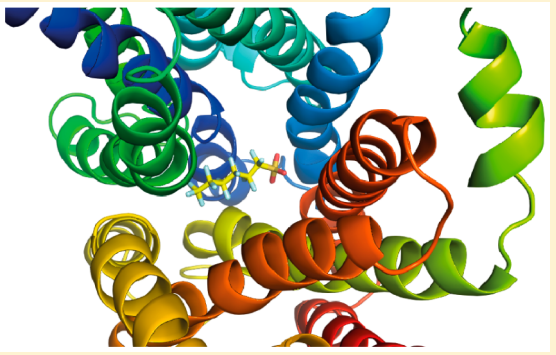

INTRODUCTION

Per- and polyfluorinated alkyl substances (PFAS) are currently of high interest in environmental science. They are used in a variety of industrial applications, from surface coatings to processing aids to fire-fighting foams.[1−4] Yet the stability of the carbon−fluorine bond—the most stable single carbon bond[5]—makes these substances environmentally problematic. Once released into the environment, remediation is difficult and costly, if not impossible.[6−9] Moreover, certain PFAS, such as long-chained perfluoroalkyl acids (PFAAs), are bioaccumulative and, in some cases, toxic.[10−12] This has led to a phasing out of PFAAs with more than six perfluorinated carbons[13−15] and to a proliferation of possible replacement substances.[16,17] However, little is known about the inherent hazards or the environmental behavior of these replacement structures. Lack of chemical standards continues to impede monitoring and experimental investigation.[18] Reliable methods to predict their behavior in the environment and organisms would be of tremendous benefit.

Recent attention on PFAS toxicokinetics has increased the study of protein interactions substantially.[19−34] In our previous work, we identified the interaction of PFAAs with proteins as important determinants of bioaccumulation potential in fish.[32] Specifically, we used binding with serum albumin, liver fatty acid binding protein, and organic anion transporters within a multicompartment toxicokinetic model to estimate the bioconcentration and tissue distribution of several perfluoroalkyl carboxylic acids (PFCAs) and perfluoroalkanesulfonic acids (PFSAs). However, the data available to validate such a model are limited to a small subset of the PFAS currently in production, exist mostly for mammalian species, and vary widely among studies.[12] Therefore, a methodology for large-scale screening of protein-PFAS interactions has not yet been developed, though some initial work indicates that in-silico docking methods may hold promise.[28,31,34]

Protein−ligand docking is an important tool in computer-aided drug design, which predicts the interaction between a protein and a ligand both in terms of structure, to find likely binding modes, and energetics, to estimate binding affinity.[35] The protein and ligand are defined by their position (x, y, z, angles) and, for the flexible ligand, by the angles of each rotatable bond. A scoring function is then used to rank possible binding modes. Deterministic or stochastic search algorithms sample a user-defined search space, "docking" the ligand in different positions and conformations to a putative binding region in the protein. Programs typically return a ranked list of best poses (those associated with the highest affinities).

In 2010, Salvalaglio et al. conducted a study combining protein−ligand docking, molecular dynamics and estimation of free energies of binding (ΔG) for perfluorooctanoic acid

Received: June 21, 2015
Revised: September 15, 2015
Accepted: September 22, 2015
Published: September 22, 2015

DOI: 10.1021/acs.est.5b03000
Environ. Sci. Technol. 2015, 49, 12306−12314

(PFOA) and perfluoroalkanesulfonic acid (PFOS) in human serum albumin (HSA).[28] They predicted the structures of PFOA-HSA and PFOS-HSA complexes and their ΔG, which indicated the strength of the bound complexes. They compared their results to the fluorescence experiments of Chen and Guo (2009), who showed that PFOA bound to the Tryptophan site (Trp) on HSA and PFOS to both the Trp site (with lower affinity than PFOA) and the Sudlow drug binding site SII (with high affinity).[36] The predicted energies for PFOS binding at Trp were similar, but higher, than the experimental values from Chen and Guo. In 2012, Luo et al. published the first crystal structure of the HSA-PFOS complex.[31] This remains the only PFAS−protein complex that has been experimentally determined to date. They show two binding sites for PFOS: fatty acid site 3/4 (FA 3/4), which overlaps with SII, and fatty acid site 6 (FA 6), which is adjacent to Trp. Salvalaglio et al. predicted a number of additional PFOA and PFOS binding sites on HSA; these have yet to be confirmed.

Zhang et al. (2013) recently investigated the binding of 17 PFAS (12 PFCAs with between 4 and 18 carbon atoms, 3 PFSAs with 4, 6, and 8 carbon atoms, and 2 fluorotelomer alcohols) to liver fatty acid binding protein (L-FABP) using a fluorescence displacement assay.[34] As a complement to this experimental technique they used molecular docking simulations to predict the conformation of the protein−ligand complexes. The simulations showed that PFAAs with more than 11 carbons cannot easily fit into the binding pocket of L-FABP, and agreed with experimentally determined K_A that decreased for chain lengths longer than 11.

Based on these recent studies, we propose that protein−ligand docking could be a useful screening tool to identify strong interactions between PFAS and proteins. Furthermore, our earlier model of PFAA bioconcentration suggests that these predicted interactions could be used as a proxy for bioaccumulation potential.[32] However, this relationship is not necessarily straightforward, since different protein interactions can influence uptake, distribution, and renal and hepatic elimination or reabsorption. It is from the balance of such interactions that complex toxicokinetic behaviors, observed at the organism level, emerge. We therefore focus this work on two questions: (1) How well do predicted K_A from docking simulations match observed K_A? (2) Is there correlation between K_A and observed toxicokinetic behavior of PFAAs?

Based on our analysis, we consider whether molecular docking tools could be used to screen for bioaccumulation potential among structurally diverse PFAS.

MATERIALS AND METHODS

Selection of Substances. In order to maximize use of available data for validation, we limit our study to perfluorinated alkyl acids (PFAAs), for which most K_A data have been collected. Because bioaccumulation data are very scarce, we use the half-life in an organism ($t_{1/2}$) as a surrogate for bioaccumulation potential. We first collected empirical K_A and $t_{1/2}$ data for linear PFCAs, linear PFSAs, and a number of branched isomers of PFOA and PFOS, for binding to HSA and/or L-FABP. This constitutes a broader set of substances with which to evaluate predicted K_A than has been previously attempted. These 25 substances are listed in Table 1. Nomenclature for isomers follows that of Benskin et al. 2010;[37] the location of branch points on the carbon chain in isomers is counted starting from the acidic headgroup.

Table 1. Perfluorinated Alkyl Acids (PFAAs) for Model-Data Comparison

name	acronym
Pefluoroalkyl Carboxylic Acids (linear)	*PFCAs*
perfluorobutanoic acid	PFBA
perfluoropentanoic acid	PFPA
perfluorohexanoic acid	PFHxA
perfluoroheptanoic acid	PFHpA
perfluorooctanoic acid	PFOA[a]
perfluorononanoic acid	PFNA
perfluorodecanoic acid	PFDA
perfluoroundecanoic acid	PFUnDA
perfluorododecanoic acid	PFDoDA
perfluorotetradecanoic acid	PFTeDA
perfluorohexadecanoic acid	PFHxDA
Pefluoroalkyl Carboxylic Acids (Branched)	
perfluoro-3-methylheptanoic acid	3m-PFOA
pefluoro-4-methylheptanoic acid	4m-PFOA
perfluoro-5-methylheptanoic acid	5m-PFOA
perfluoroisopropanoic acid	iso-PFOA
t-perfluorobutanoic acid	tb-PFOA
perfluoro-3,3-dimethylhexanoic acid	3,3m$_2$-PFOA[b]
perfluoro-4,4-dimethylhexanoic acid	4,4m$_2$-PFOA
Perfluoroalkanesulfonic Acids (Linear)	*PFSAs*
perfluorobutanesulfonic acid	PFBS
perfluorohexanesulfonic acid	PFHxS
perfluorooctanesulfonic acid	PFOS[a]
Perfluoroalkanesulfonic Acids (Branched)	
perfluoro-1-methylheptanesulfonate	1m-PFOS
perfluoro-3-methylheptanesulfonate	3m-PFOS
perfluoro-4-methylheptanesulfonate	4m-PFOS
perfluoro-5-methylheptanesulfonate	5m-PFOS
t-perfluorobutanesulfonate	tb-PFOS
perfluoroisopropanesulfonate	iso-PFOS

[a]Linear PFOA and PFOS are referred to as the n- isomers throughout the text. [b]Measured $t_{1/2}$ from a structure only tentatively identified as 3,3m$_2$-PFOA in the work of Benskin et al. (2009).

In addition, 13 linear PFCAs with 4−16 carbons and 4 linear PFSAs with 4, 6, 8, and 10 carbons were chosen for the protein docking simulations. The 45 structures used in the docking simulations can be found in the Supporting Information (SI), Table S1.

Selection of Proteins. Empirical evidence exists for the interaction of PFAAs with three classes of proteins (among other biological macromolecules): serum albmin,[24−27,30,31,36,38,39] liver fatty acid binding proteins (L-FABP),[29,34] and organic anion transporters (OATs).[40,41] For each of these protein types, 3-dimensional structural data were needed as input for protein−ligand docking. The RSCB Protein Data Bank (PDB, http://www.rcsb.org/pdb/home/home.do) contains links to structural information for more than 100 000 biological macromolecules. Files can be accessed by protein or ligand name or by their unique 4-digit alphanumeric identifiers. We searched the PDB for structures representing serum albumin, L-FABP and OATs.

Many structures were available for serum albumin. We constrained our search to human serum albumin (HSA) structures of high resolution ($\leq$ 2.5 Å). We found 31 such structures in the database. From these, we selected the subset of

DOI: 10.1021/acs.est.5b03000
Environ. Sci. Technol. 2015, 49, 12306−12314

monomeric structures (containing only one copy of the protein) and from these selected three structures based on their conformation. The first, 1E7G, is HSA complexed with myristic acid,[42] which was chosen to best represent the native structure of HSA (myristic acid is a saturated fatty acid found in many foods and animal fats and as such is likely to be complexed with HSA in the blood). The second, 4E99, is for PFOS bound to HSA, and is the only crystal structure available for HSA binding with a PFAA.[31] As Luo et al. (2012) showed in their study, HSA undergoes substantial conformational changes when binding with PFOS, becoming more compact. We then used the "align" command in PyMol[43] to measure the root-mean-square distance (RMSD) between all 31 structures, and selected a third structure to represent the midpoint between the conformations of 1E7G and 4E99. This structure, 1H9Z, is HSA complexed with myristic acid and the R+-enantiomer of Warfarin.[44] Choosing diverse structures is important because the docking program we used, Autodock Vina,[45] does not take into account conformational changes in the protein with binding. Using three different HSA structures allowed us to assess how their conformations affected interactions with different PFAAs.

For human L-FABP, only 8 structures were found in the PDB. Of these, two high-resolution structures were chosen for our study: 1LFO[46] and 3STM.[47] We chose 3STM in particular because it was also used by Zhang et al. (2013) in their study of L-FABP interaction with PFCAs.[34]

Finally, for organic anion transporters, no crystal structures are currently available. However, because these proteins and polypeptides are potentially critical in determining the half-life of PFAAs in organisms,[48] we used amino acid sequences from the Universal Protein Resource (UniProt)[49] to build estimated crystal structures with the Phyre web server (v2.0, http://www.sbg.bio.ic.ac.uk/phyre2)[50,51] for three transporters: human OAT1 and OAT3, and rat Oatp1a1. OAT1 and OAT3 mediate secretion of anions in the kidneys from the blood to the urine, while the organic anion transporting polypeptide, Oatp1a1, mediates the reabsorption of anions from the urine back to the blood; all three are known to interact with PFAAs.[40,41,52,53] Chemicals that are substrates of OAT1 or OAT3 should have lower half-lives and bioaccumulation potentials whereas those that are substrates of Oatp1a1 should have increased half-lives and bioaccumulation potentials; a chemical that interacts with both will have its elimination rate determined by the balance of these interaction strengths.[48]

Protein−Ligand Docking. We chose Autodock Vina (v1.1.2)[45] to evaluate the possibility of using a free, computationally efficient and easy-to-implement docking program for PFAA-protein interaction screening. Autodock Vina runs on a desktop computer on multiple platforms and allows for rapid screening of many structures. It requires as input files a protein structure, a ligand structure, and a conformation file with coordinates for the binding site to be explored. The protein structure files were extracted from the PDB as described above. For the PFAA ligand files, we took a "naïve" approach. 3-dimensional structures were built and structurally optimized in Avogadro (v1.1.0)[54] (which uses Open Babel force-fields for optimization) and exported in pdb format. These structures were then prepared for docking using AutoDock Tools (v1.5.6).[55] We did not take the additional steps outlined by Salvalaglio et al. (2010) to produce PFAA conformations that accurately reproduce the lowest-energy helical conformations that have been reported for perfluorinated structures.[28,56,57] This was done to test how much the docking poses and binding energies predicted by Autodock Vina, without such refinement, would deviate from experimental data. For all simulations, the deprotonated anion was docked to the protein.

The binding site boundaries were defined individually for each protein structure using the Grid menu in Autodock Tools.[55] In the case of HSA, we included six binding sites, shown in Figure S1 of the SI. These correspond to the following fatty acid binding sites (as defined by Curry[58]): FA1, FA2, FA3/4, FA5, FA6, and FA7 (SI Figure S1A). The FA3/4 site includes Sudlow's drug binding site II, and the FA7 site overlaps with Sudlow's binding site I. The Trytophan site (Trp) is located between FA6 and FA7. Grid box dimensions are listed for each HSA structure in SI Table S1.

L-FABP, OAT1, OAT3, and Oapt1a1 have only a single binding site each (SI Figure S2). In L-FABP the binding pocket has been described as a flattened rectangle;[34] in the organic anion transporters the binding pocket appears more cylindrical. Grid box dimensions used for these structures are listed in SI Table S2.

The outputs of the docking simulations are free energies of binding and docking poses. The free energy of binding (ΔG, in kcal/mol), can be translated into an equilibrium association constant (K_A, in M^{-1}) as follows:[59]

$$K_A = e^{-\Delta G/RT} \quad (1)$$

assuming a temperature of 300 K (the Autodock Vina system temperature).

We assess the success of the docking simulations in two ways. First, we redock PFOS with HSA. Redocking tests the ability of a simulation to replicate the results of an experimental binding study.[45,55] Since the only study available is the one of Luo et al. (2012),[31] we used their crystal structure of PFOS bound to HSA (PDB structure 4E99) for redocking. The root-mean-square deviation (RMSD) between the published crystal structure and the docked PFOS is calculated using the pairwise fitting procedure in PyMol.[43] An RMSD < 2 Å is considered a successful redocking.[35]

Second, we compare the estimated binding energies from our simulations to measured K_A for both HSA and L-FABP.[22,24−27,29,34,36,38,60] We assumed that the best estimate lay within the range of predicted ΔG, and used the geometric mean (GM) and geometric standard deviation (GSD) of K_A derived from these to compare with measured values. For serum albumin, an added complication is the existence of multiple binding sites. Because site-specific data were available for only very few structures, we assumed that any of the six binding regions outlined in SI Figure S1 were available for PFAA binding. We computed the GM and GSD of the K_A across all sites (54 total predictions for each chemical with HSA). For L-FABP (the only other protein for which measured K_A were available) we calculated the GM and GSD for each PFAA from the nine predicted binding affinities at the single binding site.

Lipid−Water Partition Coefficients. Lipid−water partition coefficients (K_{lw}), estimated using the COSMO*mic* membrane-water partitioning program,[61] were kindly provided by Kai Bitterman (Department of Analytical Environmental Chemistry, Helmholtz Centre for Environmental Research GmbH UFZ, Leipzig, Germany).

Correlation of K_A and K_{lw} with Half-Life Data. An ultimate goal of this study is to evaluate whether protein−ligand docking could be used to screen for PFAA bioaccumulation potential. Since we have chosen $t_{1/2}$ as a surrogate for this potential, we collected data sets for different organisms and different PFAAs. Falk et al. (2015) reported tissue-specific $t_{1/2}$ in rainbow trout for

DOI: 10.1021/acs.est.5b03000
Environ. Sci. Technol. 2015, 49, 12306−12314

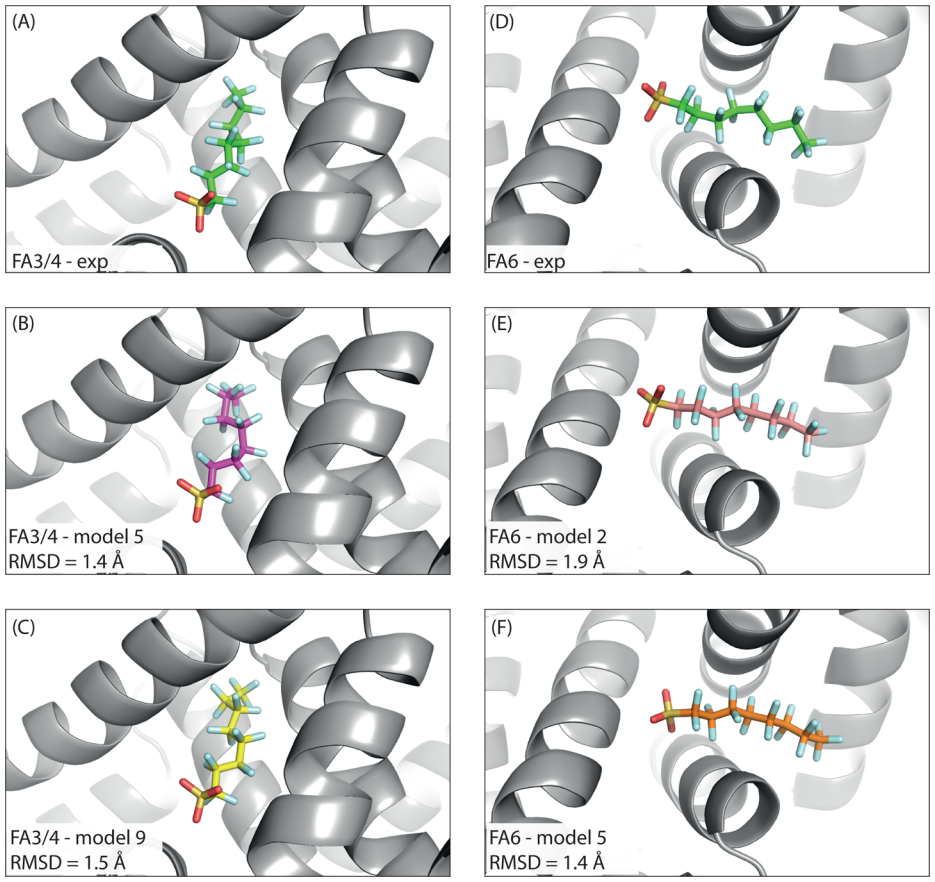

Figure 1. Comparison of docking poses for experimental and simulated PFOS interactions with human serum albumin (HSA, PDB structure 4E99), including the root mean square deviation (RMSD) between experimental and model poses. Left panel: HSA region of fatty acid binding sites 3 and 4, showing docked position of (A) experimental, (B) model pose 5 and (C) model pose 9 PFOS molecules. Right panel: HSA region of fatty acid binding site 6, showing docked position of (D) experimental, (E) model pose 2 and (F) model pose 5 PFOS molecules.

PFOA, PFNA, PFBS, PFHxS, and PFOS (no distinction made between linear and branched isomers).[62] Numata et al. (2014) reported half-life data in pigs (mixed genders) for PFHxA, PFHpA, PFOA, PFBS, PFHxS, and PFOS.[63] Zhang et al. (2013) reported elimination $t_{1/2}$ for humans (in two groups: young females and males and older females) for PFHpA, PFNA, PFDA, PFUNA, 4 PFOA isomers (*n-*, *iso-*, *4m-*, *5m-*), PFHxS, and 6 PFOS isomers (*n-*, *iso-*, *1m-*, *4m-*, *3m-*, *5m-*), as well as the sum of dimethyl PFOS isomers.[64] Benskin et al. (2009) and de Silva et al. (2009) reported blood $t_{1/2}$ in rats based on single-dose and chronic-dose studies, respectively.[65,66] Included were PFNA, PFHxS, 7 individual PFOA isomers (*n-*, *iso-*, 3m-, 4m-, 5m-, 4,4m$_2$-, and *tb-*) and 7 PFOS isomers (*n-*, *iso-*, *3m-*, *4m-*, *5m-*, and *tb-*). A few additional isomers could not be definitively identified.

We divided each data set into three subgroups and calculated the coefficient of determination (R^2) between $t_{1/2}$ and K_A for each protein for: mixed PFAAs, including only linear (or unspecified) structures; only structural isomers of PFOA; and only structural isomers of PFOS (Figure 3C). If a study distinguished between genders, we calculated correlations separately for males and females. In addition we included the K_{lw} as a measure of nonspecific membrane binding affinity, as partitioning to membrane lipids has also been suggested as a possible mechanism for PFAA bioaccumulation.[67]

Regression Analysis. We used a stepwise regression procedure to select variables important in determining $t_{1/2}$, assuming that different proteins could play different roles in whole-organism toxicokinetics. Because of variability observed between studies,[31] we used individual data sets rather than combining data from different studies, even for the same species. We evaluated models with only one structure representing each protein type (1E7G, 1H9Z or 4E99 for HSA, 1LFO or 3STM for L-FABP, OAT1 or OAT3 for OATs, plus Oatp1a1 and K_{lw}—12 possible combinations of variables for each data set). The details of this analysis can be found in SI section S6.

RESULTS AND DISCUSSION

Redocking PFOS. In Figure 1 we compare Autodock Vina simulations for PFOS with HSA (PDB structure 4E99) with the crystal structures from Luo et al. (2012).[31] The experimentally determined conformation of PFOS with HSA in the region of binding site FA3/4 is shown in Figure 1A. Autodock Vina reports the nine highest-affinity docking poses for each ligand−binding-site pair. Docking poses for FA3/4 show closest agreement for poses 5 (Figure 1B, RMSD = 1.4 Å) and 9 (Figure 1C, RMSD = 1.5 Å). For site FA6, the best predicted conformations are for model poses 2 (Figure 1E, RMSD = 1.9 Å) and 5 (Figure 1F, RMSD = 1.4 Å). All visualizations were made using PyMol.[43]

The redocking of PFOS in HSA (PDB structure 4E99) suggests that Autodock Vina can successfully predict bound conformations of PFAAs and serum albumin with reasonable accuracy (RMSD < 2 Å). The binding poses closest to the experimental results are found within the top nine results, but are not necessarily those corresponding to the highest predicted K_A.

DOI: 10.1021/acs.est.5b03000
Environ. Sci. Technol. 2015, 49, 12306−12314

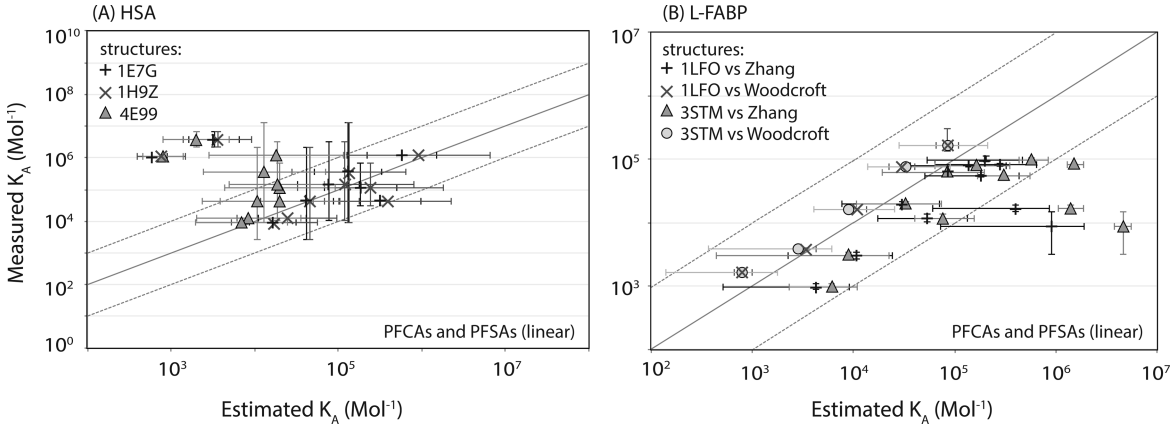

Figure 2. Comparison of measured and estimated equilibrium association constants (K_A) for linear PFAAs. Solid line represents the 1:1 line, dotted lines are a factor of 10 higher or lower. Error bars reflect one geometric standard deviation (GSD) for estimates and either GSD or range (if $n < 3$) for measured values. (A) K_A with HSA estimated using three PDB structures (1H9Z, 1E7G and 4E99) compared with the geometric mean of measured values, with estimates reduced by a factor of 20. (B) K_A with L-FABP estimated using two PDB structures (1LFO and 3STM) compared with values determined by Woodcroft et al. (2010) and Zhang et al. (2013), with estimates reduced by a factor of 20.

Predicted Equilibrium Association Constants (K_A). For linear PFAAs, measured K_A for HSA were found for the following structures: PFBA, PFHpA, PFOA, PFNA, PFDA, PFUnDA, PFDoDA, PFBS, PFHxS, and PFOS.[22,24−27,36,38,60] In Figure 2A we compare these measured association constants with the predictions from Autodock Vina, showing the GM × /÷1 GSD where possible (a number of structures had only one measured value available and thus show no vertical error bars). Clearly, both predictions and measurements are highly variable. In the case of the predicted binding strengths, the variability arises from the top 9 predicted binding affinities for each individual docking simulation (per site) and also from uncertainty as to which binding site is the "correct" one. For the measurements, very high variability has been observed due to the use of different methods and different experimental conditions (especially the protein to ligand ratio).[24,26] Predicted association constants systematically overestimated PFAA-protein binding strengths when compared with the GM of the measured values. We corrected this by dividing the K_A by 20 (equivalent to increasing ΔG by about 2 kcal/mol).

Corrected predictions using the 4E99 structure are still low compared with measured K_A (Figure 2A), whereas the predictions using 1E7G and 1H9Z are in much better agreement with the data, except for two clear outliers: PFBA and PFBS. The experimental K_A for these short-chain structures are more than 3 orders of magnitude higher than the predicted K_A. Both values come from the study of Chen and Guo (2009), and are very high compared to K_A measured in other studies for PFAAs with longer chain lengths. We think these high K_A are inconsistent with the lack of bioaccumulation generally observed for these compounds. All K_A values measured by Chen and Guo at Sudlow Sites I and II are on the order of 10^6 M^{-1}. Predicted K_A for PFUnDA, on the other hand, is a factor of 10 higher than measured by Hebert et al. (2010). All of Hebert's values (for PFHpA through PFUnDA, plus PFHxS and PFOS) were on the order of 10^4 M^{-1}. This highlights the difficulty of evaluating our predictions on such a variable set of measured data. Given the likely influence of methodology and experimental conditions on empirical K_A values, it would be ideal to compare predicted values to a series of K_A values from a single study. However, most available studies measured too few PFAAs at one time to make a useful comparison with the predicted values.

For the linear PFAAs, measured K_A were also available for association with L-FABP for: PFPA, PFHxA, PFHpA, PFOA, PFNA, PFDA, PFUnDA, PFDoDA, PFTeDA, PFHxDA, PFBS, PFHxS, and PFOS.[29,34] For the short-chain PFAAs (up to 7 perfluorinated carbons), the results of the two studies, Woodcroft et al. (2010) and Zhang et al. (2013), are in good agreement. For long-chain PFAAs only the study of Zhang et al. is available. Once again, there was a systematic overestimation of K_A by the docking simulations, which could be improved using the same adjustment factor of 20 that was used with HSA. After adjustment, we find good agreement for PFAAs up to a chain length of 9 perfluorinated carbons (that is, all of the structures included in both the Woodcroft et al. and Zhang et al. studies, plus PFNA, PFDA and PFUnDA from Zhang et al., Figure 2B). Clear outliers are PFDoDA, PFTeDA, and PFHxDA. For these structures, the GM of the docking simulations are between a factor of 18 and a factor of more than 500 higher than the measured values (for structure 3STM) and between 24 and 106 times higher than the measured values (for structure 1LFO). Thus, 1LFO appears to be a better L-FABP structure for predicting K_A, although these differences are considerably smaller for shorter-chain PFAAs.

The fact that the same factor could improve the model-data agreement for both HSA and L-FABP suggests that the docking predictions, with their highly simplified and idealized conditions, are biased toward too-strong binding. This is generally consistent with the comparison between Salvalaglio's predictions for PFOA at the Trp site[28] and the experimental observation of Chen and Guo,[36] although in that case the difference is much smaller, likely due to the more complex approach of Salvalaglio that takes molecular dynamics into account. Trott and Olson (2010) report a standard error for Autodock Vina predictions of between 2.75 and 2.85 kcal/mol;[45] our predictions for the linear PFAAs are thus well within the expected performance of this docking program. From this we infer that failure to explicitly account for the unique conformations adopted by PFAAs did not affect our predictions too negatively for short-chain PFAAs. It is likely, however, that this lack of refinement in our approach, as well as the lack of protein flexibility within Autodock Vina, affected our ability to make reasonable predictions of K_A for perfluorinated chains with more than 9 CF_2 groups.

DOI: 10.1021/acs.est.5b03000
Environ. Sci. Technol. 2015, 49, 12306−12314

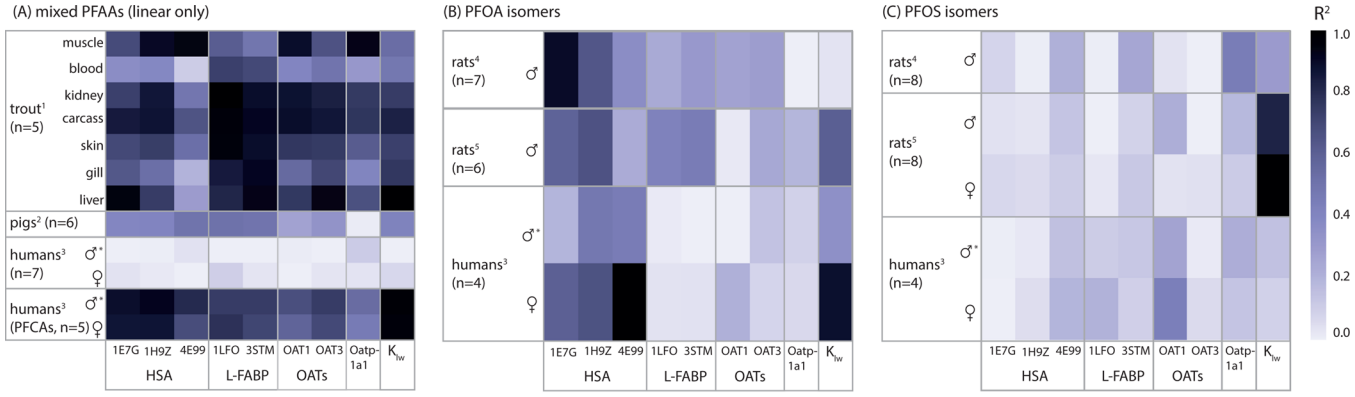

Figure 3. Correlations (R^2 values) between estimated protein binding affinity and measured PFAA half-lives in rainbow trout,[62] pigs,[63] humans,[64] and rats,[65,66] considering: (A) linear PFCAs and PFSAs, (B) PFOA isomers only, and (C) PFOS isomers only.

For the branched PFOS and PFOA isomers, too few data are available to assess model performance in a good way. Beesoon et al. (2015) recently published the first measurements of K_A between HSA and some isomers of PFOA and PFOS,[60] but this data set is still limited to three isomers for PFOS (*3m*-, *4m*- and *5m*-) and two for PFOA (*3m*- and *5m*-) in addition to the linear structures, *n*-PFOS and *n*-PFOA. Nevertheless, we illustrate the correspondence between measured and modeled K_A for these few PFOA and PFOS isomers in SI Figure S3. We also plot all predicted K_A for the 45 linear and branched PFAAs listed in SI Table S1 as a function of fluorinated carbon chain length in SI Figures S4 (for HSA), S5 (for L-FABP) and S6 (for OATs). In SI Figure S7 we plot COSMO*mic*-derived K_{lw} values for a subset of 35 of these.

Correlation with Half-Lives. The trout, pig, and human data sets contained a variety of linear PFCAs and PFSAs (Figure 3A). For humans, we created an additional group by removing PFOS and PFHxS from the data set, leaving only PFCAs. The difference between the two human data sets clearly shows that the PFSAs behave differently (we could not make the same comparison for the trout and pig data sets because two few data for each class were available). Overall, the mixed data sets show a similar correlation to different proteins and to K_{lw}. Surprisingly, for trout the reported blood $t_{1/2}$ has the lowest correlation with HSA. Except for trout muscle, structure 4E99, among the HSA structures, consistently shows the lowest correlation with $t_{1/2}$.

For the PFOA isomers (Figure 3B, including both male and female humans but only male rats, as female rats had too few data), we see that correlations with HSA are higher than with most other variables. For male rats in the single dose study,[65] correlation with HSA is highest (particularly with structure 1E7G). Correlation with K_{lw} is lowest. For male rats in the chronic dose study, on the other hand, HSA and K_{lw} have similar high R^2 values, followed by L-FABP. Correlation with OAT1 is lowest. For humans,[64] HSA and K_{lw} show highest correlation with $t_{1/2}$ for both males and females, though the R^2 values are higher for females. Correlations are lowest for L-FABP.

For the PFOS isomers (Figure 3C), correlations are generally lower than for PFOA, with the exception of the R^2 value for K_{lw} for the rats in the chronic dose study.[66] For this set, alone, R^2 values for correlation with HSA are highest for structure 4E99 for all species. Correlations with OAT3 are lowest across all species.

It is striking, considering Figure 3A in comparison with the isomers, how R^2 values for all proteins and all studies are higher when mixed PFAAs (and no isomers) are included. However, it should be noted that for linear PFAAs of increasing chain length, and particularly for the PFCAs, the differences in predicted binding strength are strongly and positively correlated with number of CF2 groups, and the same is true for K_{lw}. K_A and K_{lw} are therefore also strongly correlated. This is to be expected, since protein binding is driven by a combination of hydrophobic and polar (or electrostatic) interactions,[68−70] and the hydrophobicity of PFAAs increases with chain length. In SI Figures S11 to S15, we show correlation matrices for each study for all eight protein structures and K_{lw}. In the trout data set, for example, K_{lw} is highly and significantly correlated with HSA structures 1E7G and 1H9Z, L-FABP and OAT structures. In the pig data set, K_{lw} is highly and significantly correlated with all proteins except Oatp1a1. These patterns are generally reflected in Figure 3A.

No single variable (protein structure, K_{lw}) emerges as a "clear winner" for explaining observed patterns of $t_{1/2}$ for different PFAA classes in the different data sets. Thus, it is unlikely that a simple model that considers only partitioning or only binding to a single protein type (e.g., serum albumin) could successfully predict complex toxicokinetic behavior of PFAAs, such as elimination.

Regression Analysis for Variable Importance. We previously developed a mechanistic model for PFAA bioconcentration in trout which incorporated three kinds of protein interactions: with serum albumin, L-FABP and OATs.[32] The choice of proteins in that study was based on the availability of protein binding data. With our current approach to predicting protein binding, we wanted to know whether, by combining predicted K_A and measured $t_{1/2}$, we could identify which proteins would be most relevant for inclusion in a mechanistic bioaccumulation model, and whether K_{lw} should also be included. We therefore used the predicted K_A, the K_{lw} and the $t_{1/2}$ data for humans, rats, pigs and trout in a stepwise regression analysis, which looked for significant regression models for each data set by adding and removing proposed variables from a starting model "guess" in a sequential manner (see SI for details). Because this method often finds local minima, we varied the parameters included in the initial model and ran both forward and backward stepwise regressions.[71]

It must be emphasized here that the objective of the regression analysis was not to produce a multiple linear regression model with which to predict $t_{1/2}$ for different species. Given the large number of model parameters and small number of data-points

DOI: 10.1021/acs.est.5b03000
Environ. Sci. Technol. 2015, 49, 12306−12314

for $t_{1/2}$, the models produced are almost certainly overfitting the data. Indeed, the stepwise regression procedure is known to produce significant bias for data sets with a small number of observations and a large number of variables,[72] as we have here. Rather, we are interested in the frequency with which different proteins and K_{lw} are selected in significant regression models and whether a consistent picture emerges regarding key features that should be included in a mechanistic model.

In SI Figures S16 to S24 we show regression results for individual models including one representative for each protein group (12 models in all, see SI Table S4). Results were consistent enough to warrant merging them to get an overall picture of the importance of the different protein types and K_{lw}. In Figure 4, we show the frequency of inclusion of each variable for the different species, normalized to the maximum possible frequency (inclusion in all models). For the proteins, frequency of inclusion depended more strongly on species. For trout, L-FABP was most frequently included, while for pigs L-FABP and Oatp were included with similar frequency. For rats, HSA and L-FABP were included with similar frequency and OATs and Oatp having similar lower frequencies of inclusion. For humans, HSA was clearly present more frequently than other proteins. However, given the enormous amount of attention currently paid to studying interactions with serum albumin, the regression analysis showed a relatively low frequency of inclusion, particularly for trout.

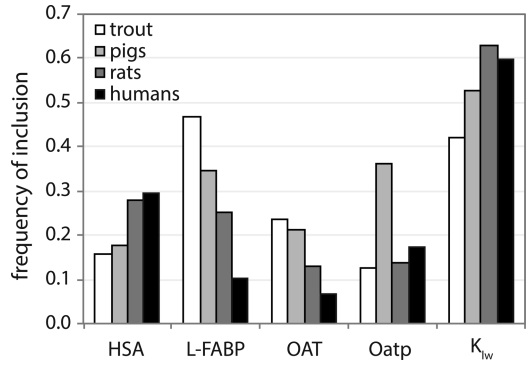

Figure 4. Frequency of variable inclusion in significant regression models (relative to maximum frequency of inclusion, all data sets by species). The category HSA includes models with 1E7G, 1H9Z, 4E99; L-FABP includes models with 1LFO or 3STM; OAT includes models with OAT1 or OAT3.

Armitage et al. (2013) proposed that partitioning of ionizable organic chemicals (including PFAAs) to membrane phospholipids could help explain their bioaccumulation and tissue distribution.[67] Our results here indicate that inclusion of phospholipid partitioning is indeed likely to be important to determining toxicokinetics of PFAAs. However, proteins show up with relatively high frequency for many of the data sets, suggesting protein interactions are also key to determining PFAA toxicokinetics. Based on the breakdown of protein frequency in these models, we propose that not enough attention is currently being paid to research on "other" proteins. While many studies have focused on the interaction of PFAS with serum albumin, L-FABP and its analogues in other tissues may actually be more important, particularly for fish.[73] Similarly, the influence of transporters like the OAT proteins and polypeptides are still very poorly understood,[74,75] yet may play an important role in determining elimination half-lives and, ultimately, bioaccumulation potential for PFAS.[40,41,48,52,53,76,77]

A Call for Data. The goal of this study was to investigate whether pharmaceutical screening tools, such as protein docking, could be used to screen for proteins that impact bioaccumulation potential of PFAS, an important class of emerging compounds. This question is challenging because binding data are still relatively limited and bioaccumulation observations are affected by many additional variables such as exposure route and amount, species, gender, and laboratory or field conditions.

The $t_{1/2}$ of a chemical in an organism is a key determinant of bioaccumulation, and is typically measured under well-controlled laboratory conditions. It has also been studied in a variety of organisms, producing a relatively rich data set (at least in the context of PFAS research) with which to test our proposals. Here, comparison of predicted K_A values with $t_{1/2}$ data from various species allowed us to expand the data with which we could assess the docking simulations, particularly with respect to PFOA and PFOS isomers. This analysis also allowed us to investigate the "higher-level" implications of protein binding for the toxicokinetics of PFAAs.

While the simple docking method we chose brings limitations in describing protein mobility or PFAA conformational accuracy, we found the greatest limitation still lay in the quality of the PFAA data—for K_A values, which are few and highly variable, and for inclusion of PFAS beyond linear PFOA and PFOS. These data limitations make validation of docking results difficult and severely restrict our ability to use statistical methods for identification of relevant model parameters. We therefore call for a broadening of work, both on PFAS−protein interactions and on their behavior in organisms. This is an enormous challenge given the wide variety of PFAS structures currently in production and the fact that analytical techniques and standards are still being developed. However, the environmental problem is also enormous. Legacy PFAAs, being highly persistent, will remain problematic in the environment for decades to come. Replacement PFAS are largely unknown quantities that need to be addressed at the earliest possible stage in order to prevent unwanted repercussions to humans and ecosystems. A concerted effort that couples computational techniques like those presented here with more robust experimental data is sorely needed.

■ ASSOCIATED CONTENT

Supporting Information

The Supporting Information is available free of charge on the ACS Publications website at DOI: 10.1021/acs.est.5b03000.

Additional text, tables and figures as noted in the text (PDF)

■ AUTHOR INFORMATION

Corresponding Author

*Phone: +41 44 633 44 92; e-mail: carla.ng@chem.ethz.ch.

Notes

The authors declare no competing financial interest.

■ ACKNOWLEDGMENTS

We thank Kai Bitterman of the Helmholtz Centre for Environmental Research (UFZ) for providing predicted K_{lw} values.

DOI: 10.1021/acs.est.5b03000
Environ. Sci. Technol. 2015, 49, 12306−12314

REFERENCES

(1) Buck, R. C.; Franklin, J.; Berger, U.; Conder, J. M.; Cousins, I. T.; de Voogt, P.; Jensen, A. A.; Kannan, K.; Mabury, S. A.; van Leeuwen, S. P. Perfluoroalkyl and polyfluoroalkyl substances in the environment: terminology, classification, and origins. *Integr. Environ. Assess. Manage.* **2011**, *7*, 513−541.

(2) D'eon, J. C.; Mabury, S. A. Is indirect exposure a significant contributor to the burden of perfluorinated acids observed in humans. *Environ. Sci. Technol.* **2011**, *45*, 7974−7984.

(3) Kannan, K. Perfluoroalkyl and polyfluoroalkyl substances: Current and future perspectives. *Env. Chem.* **2011**, *8*, 333−338.

(4) Place, B. J.; Field, J. A. Identification of novel fluorochemicals in aqueous film-forming foams used by the US military. *Environ. Sci. Technol.* **2012**, *46*, 7120−7127.

(5) Sharpe, A. G. The physical properties of the carbon-fluorine bond. *Ciba Found Symp.* **1971**, *2*, 33−54.

(6) Ahrens, L. Polyfluoroalkyl compounds in the aquatic environment: a review of their occurrence and fate. *J. Environ. Monit.* **2011**, *13*, 20−31.

(7) Houtz, E. F.; Higgins, C. P.; Field, J. A.; Sedlak, D. L. Persistence of perfluoroalkyl acid precursors in AFFF-impacted groundwater and soil. *Environ. Sci. Technol.* **2013**, *47*, 8187−8195.

(8) Simon, J. A. Editor's Perspective: Perfluorinated Chemicals Continue Gaining Momentum as an Emerging Contaminant. . *Remed J.* **2014**, *25*, 1−9.

(9) Blum, A.; Balan, S. A.; Scheringer, M.; Trier, X.; Goldenman, G.; Cousins, I. T.; Diamond, M.; Fletcher, T.; Higgins, C.; Lindeman, A. E.; et al. The Madrid Statement on Poly- and Perfluoroalkyl Substances (PFASs). *Env. Health Perspect* **2015**, *123*, A107−A111.

(10) Stahl, T.; Mattern, D.; Brunn, H. Toxicology of perfluorinated compounds. *Environ. Sci. Eur.* **2011**, *23*, 1−52.

(11) Ding, G.; Peijnenburg, W. J. Physicochemical Properties and Aquatic Toxicity of Poly- and Perfluorinated Compounds. *Crit. Rev. Environ. Sci. Technol.* **2013**, *43*, 598−678.

(12) Ng, C. A.; Hungerbuehler, K. Bioaccumulation of perfluorinated alkyl acids: observations and models. *Environ. Sci. Technol.* **2014**, *48*, 4637−4648.

(13) Vestergren, R.; Cousins, I. T. Tracking the pathways of human exposure to perfluorocarboxylates. *Environ. Sci. Technol.* **2009**, *43*, 5565−5575.

(14) Olsen, G. W.; Lange, C. C.; Ellefson, M. E.; Mair, D. C.; Church, T. R.; Goldberg, C. L.; Herron, R. M.; Medhdizadehkashi, Z.; Nobiletti, J. B.; Rios, J. A. Temporal trends of perfluoroalkyl concentrations in American Red Cross adult blood donors, 2000−-2010. *Environ. Sci. Technol.* **2012**, *46*, 6330−6338.

(15) Wang, Z.; Cousins, I. T.; Scheringer, M.; Hungerbuehler, K. Hazard assessment of fluorinated alternatives to long-chain perfluoroalkyl acids (PFAAs) and their precursors: Status quo, ongoing challenges and possible solutions. *Environ. Int.* **2015**, *75*, 172−179.

(16) Wang, S.; Huang, J.; Yang, Y.; Hui, Y.; Ge, Y.; Larssen, T.; Yu, G.; Deng, S.; Wang, B.; Harman, C. First report of a Chinese PFOS alternative overlooked for 30 years: its toxicity, persistence, and presence in the environment. *Environ. Sci. Technol.* **2013**, *47*, 10163−10170.

(17) D'Agostino, L. A.; Mabury, S. A. Identification of novel fluorinated surfactants in aqueous film forming foams and commercial surfactant concentrates. *Environ. Sci. Technol.* **2014**, *48*, 121−129.

(18) Valsecchi, S.; Rusconi, M.; Polesello, S. Determination of perfluorinated compounds in aquatic organisms: a review. *Anal. Bioanal. Chem.* **2013**, *405*, 143−157.

(19) Vandenheuvel, J. P.; Kuslikis, B. I.; Peterson, R. E. Covalent binding of perfluorinated fatty-acids to proteins in the plasma, liver and testes of rats. *Chem.-Biol. Interact.* **1992**, *82*, 317−328.

(20) Luebker, D. J.; Hansen, K. J.; Bass, N. M.; Butenhoff, J. L.; Seacat, A. M. Interactions of fluorochemicals with rat liver fatty acid-binding protein. *Toxicology* **2002**, *176*, 175−185.

(21) Jones, P. D.; Hu, W. Y.; De, C.; Newsted, J. L.; Giesy, J. P. Binding of perfluorinated fatty acids to serum proteins. *Environ. Toxicol. Chem.* **2003**, *22*, 2639−2649.

(22) Han, X.; Snow, T. A.; Kemper, R. A.; Jepson, G. W. Binding of perfluorooctanoic acid to rat and human plasma proteins. *Chem. Res. Toxicol.* **2003**, *16*, 775−781.

(23) Weiss, J. M.; Andersson, P. L.; Lamoree, M. H.; Leonards, P. E.; van Leeuwen, S. P.; Hamers, T. Competitive binding of poly-and perfluorinated compounds to the thyroid hormone transport protein transthyretin. *Toxicol. Sci.* **2009**, *109*, 206−216.

(24) Bischel, H. N.; MacManus-spencer, L. A.; Luthy, R. G. Noncovalent interactions of long-chain perfluoroalkyl acids with serum albumin. *Environ. Sci. Technol.* **2010**, *44*, 5263−5269.

(25) Hebert, P. C.; MacManus-spencer, L. A. Development of a fluorescence model for the binding of medium- to long-chain perfluoroalkyl acids to human serum albumin through a mechanistic evaluation of spectroscopic evidence. *Anal. Chem.* **2010**, *82*, 6463−6471.

(26) MacManus-Spencer, L. A.; Tse, M. L.; Hebert, P. C.; Bischel, H. N.; Luthy, R. G. Binding of perfluorocarboxylates to serum albumin: A comparison of analytical methods. *Anal. Chem.* **2010**, *82*, 974−981.

(27) Qin, P.; Liu, R.; Pan, X.; Fang, X.; Mou, Y. Impact of carbon chain length on binding of perfluoroalkyl acids to bovine serum albumin determined by spectroscopic methods. *J. Agric. Food Chem.* **2010**, *58*, 5561−5567.

(28) Salvalaglio, M.; Muscionico, I.; Cavallotti, C. Determination of energies and sites of binding of PFOA and PFOS to human serum albumin. *J. Phys. Chem. B* **2010**, *114*, 14860−14874.

(29) Woodcroft, M. W.; Ellis, D. A.; Rafferty, S. P.; Burns, D. C.; March, R. E.; Stock, N. L.; Trumpour, K. S.; Yee, J.; Munro, K. Experimental characterization of the mechanism of perfluorocarboxylic acids' liver protein bioaccumulation: The key role of the neutral species. *Environ. Toxicol. Chem.* **2010**, *29*, 1669−1677.

(30) Bischel, H. N.; MacManus-spencer, L. A.; Zhang, C. J.; Luthy, R. G. Strong associations of short-chain perfluoroalkyl acids with serum albumin and investigation of binding mechanisms. *Environ. Toxicol. Chem.* **2011**, *30*, 2423−2430.

(31) Luo, Z. P.; Shi, X. L.; Hu, Q.; Zhao, B.; Huang, M. D. Structural evidence of perfluorooctane sulfonate transport by human serum albumin. *Chem. Res. Toxicol.* **2012**, *25*, 990−992.

(32) Ng, C. A.; Hungerbühler, K. Bioconcentration of perfluorinated alkyl acids: how important is specific binding? *Environ. Sci. Technol.* **2013**, *47*, 7214−7223.

(33) Rand, A. A.; Mabury, S. A. Covalent Binding of Fluorotelomer Unsaturated Aldehydes (FTUALs) and Carboxylic Acids (FTUCAs) to Proteins. *Environ. Sci. Technol.* **2013**, *47*, 1655−1663.

(34) Zhang, L.; Ren, X. M.; Guo, L. H. Structure-based investigation on the interaction of perfluorinated compounds with human liver fatty acid binding protein. *Environ. Sci. Technol.* **2013**, *47*, 11293−11301.

(35) Morris, G. M.; Lim-Wilby, M. Molecular docking. *Methods Mol. Biol.* **2008**, *443*, 365−382.

(36) Chen, Y. M.; Guo, L. M. Fluorescence study on site-specific binding of perfluoroalkyl acids to human serum albumin. *Arch. Toxicol.* **2009**, *83*, 255−261.

(37) Benskin, J. P.; Silva, A. O. D.; Martin, J. W. Isomer Profiling of Perfluorinated Substances as a Tool for Source Tracking: A Review of Early Findings and Future Applications. In *Reviews of Environmental Contamination and Toxicology*; Voogt, P. D., Ed.; Springer: New York, 2010; Vol. *208*, pp 111−160.

(38) Wu, L. L.; Gao, H. W.; Gao, N. Y.; Chen, F. F.; Chen, L. Interaction of perfluorooctanoic acid with human serum albumin. *BMC Struct. Biol.* **2009**, *9*, 31.

(39) Zhang, X.; Chen, L.; Fei, X. C.; Ma, Y. S.; Gao, H. W. Binding of PFOS to serum albumin and DNA: insight into the molecular toxicity of perfluorochemicals. *BMC Mol. Biol.* **2009**, *10*, 16.

(40) Weaver, Y. M.; Ehresman, D. J.; Butenhoff, J. L.; Hagenbuch, B. Roles of rat renal organic anion transporters in transporting perfluorinated carboxylates with different chain lengths. *Toxicol. Sci.* **2010**, *113*, 305−314.

(41) Yang, C.-H.; Glover, K. P.; Han, X. Organic anion transporting polypeptide (Oatp) 1a1-mediated perfluorooctanoate transport and evidence for a renal reabsorption mechanism of Oatp1a1 in renal

DOI: 10.1021/acs.est.5b03000
Environ. Sci. Technol. 2015, 49, 12306−12314

elimination of perfluorocarboxylates in rats. *Toxicol. Lett.* **2009**, *190*, 163−171.
(42) Bhattacharya, A. A.; Grüne, T.; Curry, S. Crystallographic analysis reveals common modes of binding of medium and long-chain fatty acids to human serum albumin. *J. Mol. Biol.* **2000**, *303*, 721−732.
(43) Schrodinger, L. L. C. The PyMOL Molecular Graphics System, Version 1.7.2.1. August 2010.
(44) Petitpas, I.; Bhattacharya, A. A.; Twine, S.; East, M.; Curry, S. Crystal structure analysis of warfarin binding to human serum albumin: anatomy of drug site I. *J. Biol. Chem.* **2001**, *276*, 22804−22809.
(45) Trott, O.; Olson, A. J. AutoDock Vina: improving the speed and accuracy of docking with a new scoring function, efficient optimization, and multithreading. *J. Comput. Chem.* **2010**, *31*, 455−461.
(46) Thompson, J.; Winter, N.; Terwey, D.; Bratt, J.; Banaszak, L. The crystal structure of the liver fatty acid-binding protein. A complex with two bound oleates. *J. Biol. Chem.* **1997**, *272*, 7140−7150.
(47) Sharma, A.; Sharma, A. Fatty acid induced remodeling within the human liver fatty acid-binding protein. *J. Biol. Chem.* **2011**, *286*, 31924−31928.
(48) Han, X.; Nabb, D. L.; Russell, M. H.; Kennedy, G.; Rickard, R. Renal Elimination of Perfluorocarboxylates (PFCAs). *Chem. Res. Toxicol.* **2012**, *25*, 35−46.
(49) UniProtConsortium. UniProt: A hub for protein information. *Nucleic Acids Res.* **2015**, *43*, D204−D212.10.1093/nar/gku989
(50) Kelley, L. A.; Sternberg, M. J. E. Protein structure prediction on the Web: a case study using the Phyre server. *Nat. Protoc.* **2009**, *4*, 363−371.
(51) Kelley, L. A.; Mezulis, S.; Yates, C. M.; Wass, M. N.; Sternberg, M. J. The Phyre2 web portal for protein modeling, prediction and analysis. *Nat. Protoc.* **2015**, *10*, 845−858.
(52) Katakura, M.; Kudo, N.; Tsuda, T.; Hibino, Y.; Mitsumoto, A.; Kawashima, Y. Rat organic anion transporter 3 and organic anion transporting polypeptide 1 mediate perfluorooctanoic acid transport. *J. Health Sci.* **2007**, *53*, 77−83.
(53) Nakagawa, H.; Hirata, T.; Terada, T.; Jutabha, P.; Miura, D.; Harada, K. H.; Inoue, K.; Anzai, N.; Endou, H.; Inui, K. Roles of organic anion transporters in the renal excretion of perfluorooctanoic acid. *Basic Clin. Pharmacol. Toxicol.* **2008**, *103*, 1−8.
(54) Hanwell, M. D.; Curtis, D. E.; Lonie, D. C.; Vandermeersch, T.; Zurek, E.; Hutchison, G. R. Avogadro: an advanced semantic chemical editor, visualization, and analysis platform. *J. Cheminf.* **2012**, *4*, 17.
(55) Morris, G. M.; Huey, R.; Lindstrom, W.; Sanner, M. F.; Belew, R. K.; Goodsell, D. S.; Olson, A. J. AutoDock4 and AutoDockTools4: Automated docking with selective receptor flexibility. *J. Comput. Chem.* **2009**, *30*, 2785−2791.
(56) Zhang, X.; Lerner, M. M. Structural refinement of the perfluorooctanesulfonate anion and its graphite intercalation compounds. *Phys. Chem. Chem. Phys.* **1999**, *1*, 5065−5069.
(57) Jang, S. S.; Blanco, M.; Goddard, W. A.; Caldwell, G.; Ross, R. B. The source of helicity in perfluorinated N-alkanes. *Macromolecules* **2003**, *36*, 5331−5341.
(58) Curry, S. Plasma albumin as a fatty acid carrier. *Adv. Molec Cell Biol.* **2003**, *33*, 29−46.
(59) Caldwell, G. W.; Yan, Z. Y. Isothermal titration calorimetry characterization of drug-binding energetics to blood proteins. In *Optimization in Drug Discovery: in Vitro Methods*, Methods in Pharmacology and Toxicology; Yan, Z., Caldwell, G. W., Eds.; Humana Press, Inc: Totowa, NJ, 2004; pp 123−149.
(60) Beesoon, S.; Martin, J. W. Isomer-Specific Binding Affinity of Perfluorooctanesulfonate (PFOS) and Perfluorooctanoate (PFOA) to Serum Proteins. *Environ. Sci. Technol.* **2015**, *49*, 5722−5731.
(61) Bittermann, K.; Spycher, S.; Endo, S.; Pohler, L.; Huniar, U.; Goss, K. U.; Klamt, A. Prediction of Phospholipid-Water Partition Coefficients of Ionic Organic Chemicals Using the Mechanistic Model COSMOmic. *J. Phys. Chem. B* **2014**, *118*, 14833−14842.
(62) Falk, S.; Failing, K.; Georgii, S.; Brunn, H.; Stahl, T. Tissue specific uptake and elimination of perfluoroalkyl acids (PFAAs) in adult rainbow trout (Oncorhynchus mykiss) after dietary exposure. *Chemosphere* **2015**, *129*, 150−156.
(63) Numata, J.; Kowalczyk, J.; Adolphs, J.; Ehlers, S.; Schafft, H.; Fuerst, P.; Mu ller-Graf, C.; Lahrssen-Wiederholt, M.; Greiner, M. Toxicokinetics of seven perfluoroalkyl sulfonic and carboxylic acids in pigs fed a contaminated diet. *J. Agric. Food Chem.* **2014**, *62*, 6861−6870.
(64) Zhang, Y.; Beesoon, S.; Zhu, L.; Martin, J. W. Biomonitoring of perfluoroalkyl acids in human urine and estimates of biological half-life. *Environ. Sci. Technol.* **2013**, *47*, 10619−10627.
(65) Benskin, J. P.; De Silva, A. O.; Martin, L. J.; Arsenault, G.; McCrindle, R.; Riddell, N.; Mabury, S. A.; Martin, J. W. Disposition of perfluorinated acid isomers in sprague-dawley rats; Part 1: Single dose. *Environ. Toxicol. Chem.* **2009**, *28*, 542−554.
(66) De Silva, A. O.; Benskin, J. P.; Martin, L. J.; Arsenault, G.; McCrindle, R.; Riddell, N.; Martin, J. W.; Mabury, S. A. Disposition of perfluorinated acid isomers in sprague-dawley rats; Part 2: Subchronic dose. *Environ. Toxicol. Chem.* **2009**, *28*, 555−567.
(67) Armitage, J. M.; Arnot, J. A.; Wania, F.; Mackay, D. Development and evaluation of a mechanistic bioconcentration model for ionogenic organic chemicals in fish. *Environ. Toxicol. Chem.* **2013**, *32*, 115−128.
(68) Fasano, M.; Curry, S.; Terreno, E.; Galliano, M.; Fanali, G.; Narciso, P.; Notari, S.; Ascenzi, P. The extraordinary ligand binding properties of human serum albumin. *IUBMB Life* **2005**, *57*, 787−796.
(69) Ghuman, J.; Zunszain, P. A.; Petitpas, Ib.; Otagiri, M.; Curry, S. Structural basis of the drug-binding specificity of human serum albumin. *J. Mol. Biol.* **2005**, *353*, 38−52.
(70) Lexa, K. W.; Dolghih, E.; Jacobson, M. P. A Structure-based model for predicting serum albumin binding. *PLoS One* **2014**, *9*, 9.
(71) Hauck, W. W.; Miike, R. A proposal for examining and reporting stepwise regressions. *Stat Med.* **1991**, *10*, 711−715.
(72) Steyerberg, E. W.; Eijkemans, M. J.; Habbema, J. D. F. Stepwise selection in small data sets: a simulation study of bias in logistic regression analysis. *J. Clin Epidemiol* **1999**, *52*, 935−942.
(73) Chuang, S.; Velkov, T.; Horne, J.; Porter, C. J.; Scanlon, M. J. Characterization of the drug binding specificity of rat liver fatty acid binding protein. *J. Med. Chem.* **2008**, *51*, 3755−3764.
(74) VanWert, A. L.; Gionfriddo, M. R.; Sweet, D. H. Organic anion transporters: discovery, pharmacology, regulation and roles in pathophysiology. *Biopharm. Drug Dispos.* **2010**, *31*, 1−71.
(75) Hagenbuch, B.; Stieger, B. The SLCO (former SLC21) superfamily of transporters. *Mol. Aspects Med.* **2013**, *34*, 396−412.
(76) Yang, C.-H.; Glover, K. P.; Han, X. Characterization of cellular uptake of perfluorooctanoate via organic anion-transporting polypeptide 1A2, organic anion transporter 4, and urate transporter 1 for their potential roles in mediating human renal reabsorption of perfluorocarboxylates. *Toxicol. Sci.* **2010**, *117*, 294−302.
(77) König, J.; Müller, F.; Fromm, M. F. Transporters and drug-drug interactions: important determinants of drug disposition and effects. *Pharmacol. Rev.* **2013**, *65*, 944−966.

DOI: 10.1021/acs.est.5b03000
Environ. Sci. Technol. 2015, 49, 12306−12314